

ONE-POT SYNTHESIS OF CHITOSAN@CoFe₂O₃-GRAPHENE OXIDENANOCOMPOSITES AS ELECTRODE MATERIALS FOR ELECTROCHEMICAL BIOSENSOR AND SUPER CAPACITOR

C. VANITHA^a, M. SUCHARITHA^b, S. ANANDHAVELU^{a,*},
V. SETHURAMAN^a, A. YOGANANTH^c

^a*Department of Chemistry, Vel Tech Multi Tech Dr.Rangarajan Dr.Sakunthala Engineering College, Avadi, Chennai-600062*

^b*Department of Electronics Communication and Engineering, Malla Reddy College of Engineering and Technology, Maisammaguda, Secunderabad*

^c*Department of Chemistry, King Nandhivarman college of Arts and Science, Vandavasi, Thellar-604406*

In this work, a facile and low-cost method for preparation of the chitosan@ CoFe₂O₃ - Graphene oxide hybrid nanocomposites using biopolymer Chitin, Cobalt chloride and Ferrous chloride in presence of sodium hydroxide solution. FTIR and UV-vis spectra are confirmed by functional groups. XRD patterns revealed the mixture of hexagonal and tetragonal phase polycrystalline of CoFe₂O₃/Graphene oxidenanocomposites exhibited with predominant lattice plane. The average crystalline size of CoFe₂O₃/Graphene oxidenanocomposites was estimated at ~15.2 nm by Debye-Scherrer's formula. The surface morphology was demonstrated by FESEM. The shape and size of the grains were discovered by TEM analysis. The elemental composition ratio of CoFe₂O₃/Graphene oxide nanocomposites was studied by EDX analysis. The fabricated sensor investigated shows a maximum current response at pH 7.0. The L-dopa sensor exhibited wide sensing linear range from 1×10^{-7} to 3×10^{-5} M and the lower detection limit of 0.5×10^{-7} M. Conductivity and super capacitance was measured by Impedence Spectroscopy (IS) and Galvanostatic charge/discharging process.

(Received November 29, 2019; Accepted February 6, 2021)

Keywords: Nanocomposites, TEM, Supercapacitor, FESEM, Iron oxide

1. Introduction

Over the past few years, considerable effort has been devoted to the development of alternative energy storage/conversion devices with high power and energy densities because of the ever-increasing environmental problems and the up-coming depletion of fossil fuels [1-3]. As an intermediate system between dielectric capacitors and batteries, supercapacitors have attracted a great deal of attention owing to their higher power densities relative to secondary batteries and traditional electric double-layer capacitors [4,5]. The research on carbon nanotubes (CNTs) has drawn great attention because of their widespread applications in fields such as catalysts, sensors, supercapacitors, and so on [6].

Recently the study of graphene became another hot topic owing to their monolayer arrangement of carbon atoms in a honeycomb network, which can be considered as an unrolled CNT [7-9]. Graphene oxide (GO), one of the most important derivatives of graphene, is characterized by a layered structure with oxygen functional groups bearing on the basal planes and edges [10-13]. The utilization of n various carbonaceous materials, such as activated carbons, carbon fibers, and CNTs, as the electrode materials for supercapacitors has been investigated extensively [14-17]. However, to the best of our knowledge, little work has been carried out on the application of GOs in supercapacitors [18-20]. Generally, there are two types of supercapacitors based on the electrode materials: (1) high surface area, inert and conductive materials that store and release energy by nanoscopic charge separation at the electrochemical interface between an

* Corresponding author: sranand2204@gmail.com

electrode and an electrolyte and (2) some redox active materials that use fast, reversible redox reactions at the surface of active materials, which is known as the pseudo capacitance. The carbonaceous nanostructures (like CNTs, active carbon, and graphene) are commonly studied as electrodes for electrochemical double layer capacitors (EDLCs); while transition metal oxides, including MnO_2 , are promising material for pseudocapacitors.

In this work, we aimed to prepare chitosan@ CoFe_2O_3 - Graphene oxidenanocomposites from chitin as bio surfactant, cobalt chloride, iron oxide and Graphene oxide as source materials in presence of sodium hydroxide as precipitating agent using chitin deacetylation method. For this conversion of chitin into Cobalt doped graphene oxide- Fe_2O_3 composite were characterized by the functional group using FTIR and UV-Vis spectroscopy, crystallite size and phase identified by XRD. Surface morphology and size in nano is analysed by SEM and TEM. Super Capacitance performance was analysed using Charge/discharge studies. The L-dopa sensor exhibited wide sensing linear range from 1×10^{-8} to $3 \times 10^{-5}\text{M}$ and the lower detection limit of $0.5 \times 10^{-8}\text{M}$.

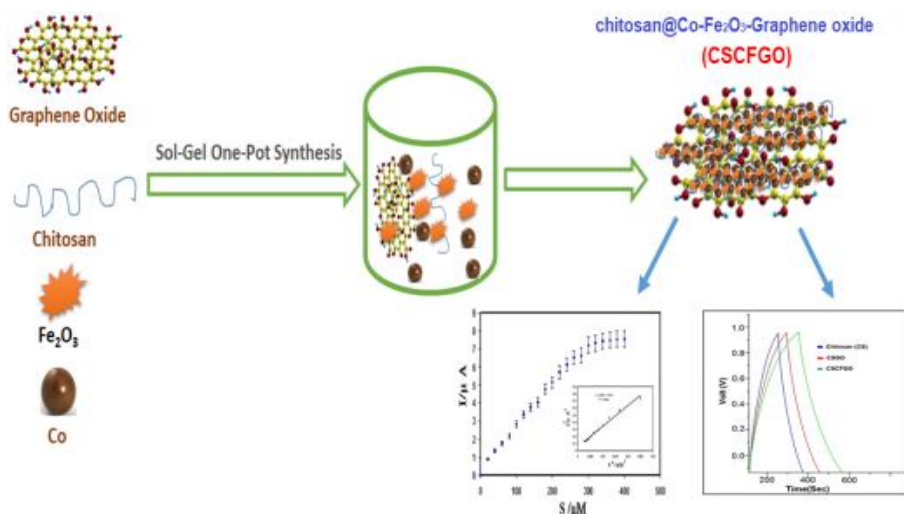
2. Experimental details

2.1. Chemicals

Graphite flakes, sulphuric acid, hydrogen peroxide, potassium dichromate, potassium permanganate, ferric chloride, cobalt chloride, L-dopa and all the solution are prepared by double distilled water. Graphene oxide was prepared by modified hummer's method [21].

2.2 Preparation of chitosan@ CoFe_2O_3 -GO hybrid nanocomposites

Exactly 0.5g of chitin was dissolved in 5 ml of acetic acid separately and then the solution was heated at 70°C and stirred well by using magnetic stirrer for about 15 min. To this (15% of 50ml) Cobalt chloride, Fe_2O_3 and 20ml of graphene oxide was added to the above mixture. It was allowed to stand for 2 hr constant stirring at maintain 70°C temperature. Then the solution was cooled and (30% of 50ml) sodium hydroxide solution was added in micro-addition. Then the precipitate was formed and left undisturbed for 24 hr. The supernatant solution was discarded and the remaining formed precipitate was allowed to settle for 24 hr by adding 400 ml of deionized water. The washing was repeated for several times. Then the clear solution was removed and the remaining precipitate was filtered using suction pump and dried in the oven at 110°C for 2 hr. The sample was ground in mortar and it designated as CSCFGO are shown in Scheme.1. The same process was repeated without addition of and Cobalt and Iron oxidesolution was added. The sample is designated as CSGO.



Scheme.1. Synthesis of Chitosan@ $\text{Co-Fe}_2\text{O}_3$ -Graphene oxide hybrid composites

2.3. Fabrication of Charge-Discharge

A mixture of 80 wt% of the materials, 10 wt% of acetylene black and 10 wt% of polyvinylidene difluoride (PVdF) as a binder with a weight ratio of 80:10:10 were sufficiently mixed in 3 ml of N-methyl-2-pyrrolidone (NMP) solvent as a paste. This paste was coated onto the stainless steel (1 cm²) electrode and dried in an oven at 110°C for overnight before the electrochemical test. This served as the working electrode. Three electrode cell systems were used to evaluate the electrochemical performance by electrochemical impedance spectroscopy (EIS), cyclic voltammetry (CV) and galvanostatic charge-discharge techniques (Autolab-BSTR 10A) at room temperature. The electrolyte was used as a 0.2 M H₂SO₄ aqueous solution. A platinum and saturated calomel electrode (SCE) was used as a counter and reference electrodes, respectively.

2.4. Fabrication of electrochemical sensor

For the voltammetric studies, a 3 mm diameter glassy carbon as a working electrode, platinum wire auxiliary and Ag/AgCl as a reference electrode. Stock solutions of L-dopa were freshly prepared by appropriate buffer solutions with 0.1 M. Aqueous solutions were prepared using doubled distilled water and all solutions were deaerated by purging with high pure nitrogen gas for all experiments. All experiments were carried out at room temperature (25 ± 2 °C). The GCE was modified using Au for the enhancement of conductivity and to attain very good porous nature of the electrode. These functions are controlled through CHI 760C software. In order to get reproducible results great care was exercised in the electrode pre-treatment. 1 mg of prepared composite in distilled water was prepared about 10 mL and shaken well 15 min using shaker. 10 μL of the mixture was drop casted over the glassy carbon electrode and dried at 4°C. Finally, the electrode was washed with the same buffer to remove loosely bounded composite material on the electrode surface.

3. Results and discussion

3.1. Fourier transforms infrared

FTIR spectrum of chitosan@ Co-Fe₂O₃ - Graphene oxide composite is shown in (Fig. 1a - b). The characteristic peak appeared at 3490 cm⁻¹, which is attributed to the OH stretching vibration. The peak appeared at 2924 cm⁻¹ corresponds to C-H stretching vibration. The peak observed at 1651 cm⁻¹ which is attributed to the NH stretching vibration from primary amines and of low intensity from C-H bond of the CH₂ bending vibration peak appeared at 1368 cm⁻¹. The small contents of residual acetamide group found in the polymeric chain as a consequence of incomplete deacetylation of chitosan. The symmetric stretching vibration of C-O-C group appeared at 1192 cm⁻¹. The stretching vibration of C-O group appeared at 1115 cm⁻¹. The band at 652 cm⁻¹ corresponds to N-H wagging vibration. The band at 599 cm⁻¹ corresponds to C-H bending vibration. The stretching vibration peak appeared at 447 cm⁻¹ corresponds to Co-Fe₂O₃ groups.

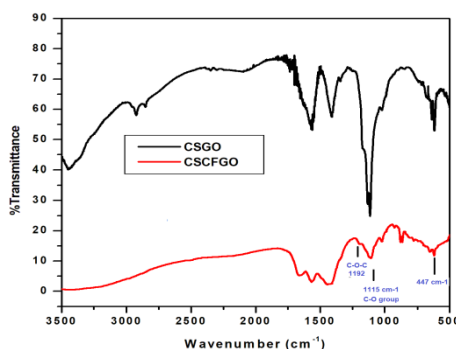


Fig.1. FTIR spectra of (a) CSGO composite (b) CSCFGO composite.

3.2. UV-Visible spectroscopy

The UV-Vis spectra of the chitosan@ Co-Fe₂O₃ - Graphene oxide hybrid composite are shown in (Fig.2). The CSGO composite is having Graphene oxide, Chitin and sodium hydroxide. The absorbance of CSCFGO composite was observed the two peaks at 210 (chitosan) and 290-380 nm (red colour-low absorbance). This is due to the presence of Co-Fe₂O₃ composite.

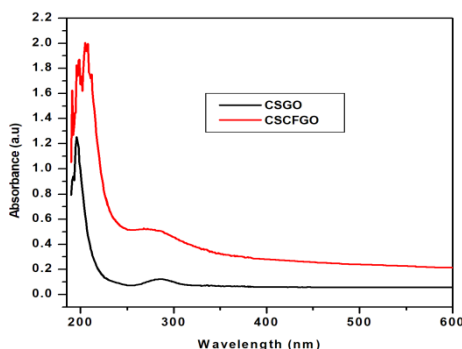


Fig. 2. UV-Visible spectra of (a) CSGO composite (b) CSCFGO composite.

The UV-Vis spectrum of the **CSCFGO composite** is shown in (Fig.2b). The composite is having Cobalt chloride, Iron oxide, Graphene oxide and sodium hydroxide with chitin. The absorbance of chitosan-Graphene oxide composite was observed two peaks at 211 (chitosan) and 290 nm (high absorbance). The UV-Vis spectrum of the Co-Fe₂O₃ composite is shown in (Fig. 2b), we concluded that the presence of Co and Fe₂O₃ in the composites.

3.3. XRD analysis

The XRD pattern of chitosan@ Co-Fe₂O₃ - Graphene oxide hybrid nanocomposites are shown in (Fig. 3). The refined unit cell parameters ($a=5.091 \text{ \AA}$, $b=8.791 \text{ \AA}$ and $c=9.430 \text{ \AA}$) are confirmed well to the reported values of $a=5.095 \text{ \AA}$, $b=8.789 \text{ \AA}$ and $c=9.437 \text{ \AA}$. The average size of the as-synthesized crystalline Fe₂O₃ calculated from the half-width of the (122) diffraction peak using the Scherrer formula is 16.54 nm (Fig.3a). X-ray diffraction patterns of Co nanostructures are obtained at different molar ratio concentrations as shown in Fig.3b. The average size of the as-synthesized crystalline Co calculated from the half-width of the (111) diffraction peak using the Scherrer formula is 19 nm.

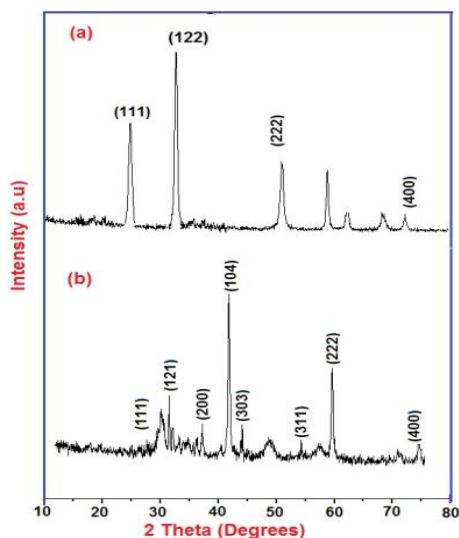


Fig. 3. XRD pattern of (a) CSCFGO (b) CSGO Composite.

3.4. Surface morphology

Fig. 4 (a-b)) show the SEM image of chitosan@ Co-Fe₂O₃- Graphene oxide hybrid nanocomposite. The surface morphology of sample (CSGO) was observed the agglomeration of composite. It has been number of particles and much bigger in particles so it is not nanometer in size. This image observed may be composite chitosan easily form the chelation to the metal oxide so surface from composite. The HR-TEM images of chitosan/graphene oxide bionanocomposite are shown in Fig. 4(c-d) indicates a strong interaction between the chitosan and graphene oxide. We observed in image folds and wrinkle nature at the rim of the graphene oxide due to intrinsic 2 thermodynamically unstable properties [21]. It is clearly visible in the image that 3 chitosan biopolymer is uniformly coated on the surface of graphene sheets.

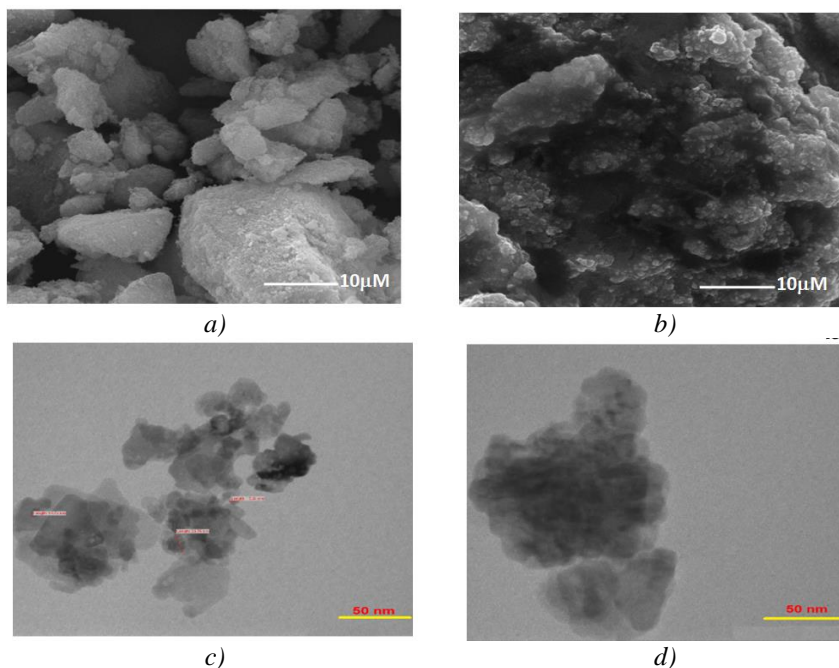


Fig. 4. SEM image of (a) CSGO and (b) CSCFGO, TEM images of (c) CSGO and (d) CSCFGO hybrid nanocomposites.

3.5. EDAX Analysis

This image is clearly shows the surface is made up of composite. (Fig.5) shows that EDAX analysis of Chitosan@Co-Fe₂O₃. Graphene oxide hybrid nanocomposite. The atomic ratio of hybrid composites (Co:Fe₂O₃) 1:1 is believed that ratio of Co and Fe₂O₃ nanocomposites.

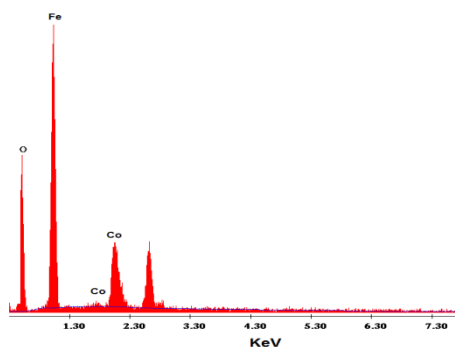


Fig.5. EDAXof analysis of CSCFGO hybrid nanocomposites.

3.6. Supercapacitor characterization Studies

Impedance spectroscopy (IS), Cyclic Voltammetry and charge discharge studies of the composites (CSGO) and hybrid composites (CSCFGO) is shown in Fig. 6 (A-B). A composite CSGO is observed in the linear high frequency region. The resistance charge transfer (R_{ct}) and conductivity values are $0.1423 \text{ M}\Omega$ and $4.25 \times 10^{-6} \text{ S/cm}$, respectively. For the hybrid composite of CSCFGO, it is noted that the R_{ct} decreased ($0.1368 \text{ M}\Omega$) and the conductivity increased to $7.69 \times 10^{-6} \text{ S/cm}$ due to the presence of Cobalt and Iron oxide in the composite. The IS spectra of the hybrid composite CSCFGO show that the straight line is increased slightly compared to that of CSGO. In the hybrid composites CSCFGO shows higher value because CS, Fe_2O_3 , Cobalt and GO play a major role in the conductivity properties.

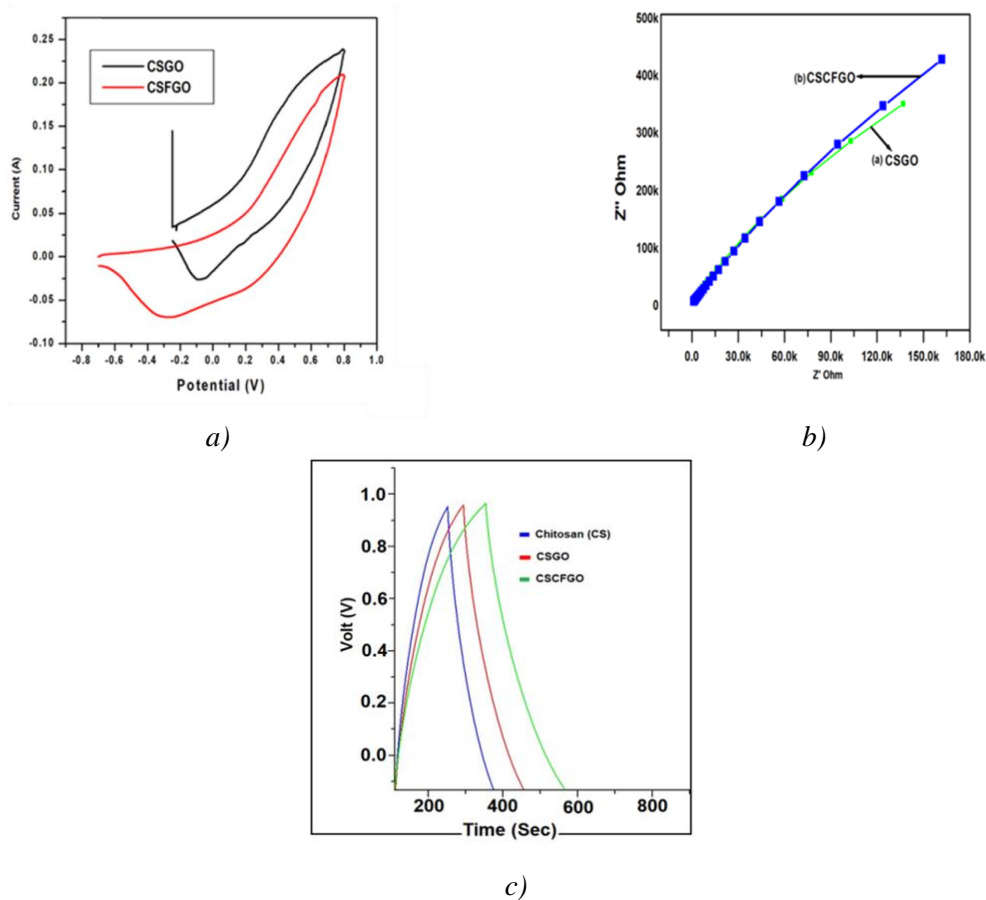


Fig. 6.(A) Cyclic Voltammetry studies of (a) CSGO (b) CSCFGO Composite, (B) IS spectra of (a) CSGO (b) CSCFGO Composite and (C) Galvanostatic charge/discharge cycling curves of (a) Chitosan (CS), (b) CSGO and (c) CSCFGO Composite.

Galvanostatic charge/discharge is a commonly used way in electrochemical capacitor study, information such as capacitance and long cycle capability of electrode materials can be obtained based on these experiments [11].

The average specific capacitance values, C_{avg} (F g^{-1}) of the samples are estimated from the discharge process according to the following equation.

$$C_g = I\Delta t/\Delta V \times m \quad (1)$$

where I is the current loaded (A), Δt is the discharge time (s), ΔV is the potential change during discharge process, and m is the mass of the active material in a single electrode (g). The representative charge/discharge curves at a current density of 0.1 A g^{-1} are shown in (Fig.6C).

Though, the CSGO exhibiting comparatively better performance than others, the stability of the CS is not appreciable. Thus, the composite CSCFGO has exhibiting superior performance in terms of stability. It can be seen that the charge curves almost linear and symmetrical to their discharge counterparts, indicating good electrochemical performance of the CSCFGO hybrid composites.

3.7. Biosensor characterization studies

The electrochemical behavior was investigated using cyclic voltammetry at GCE modified electrode CSCFGO to find out charge-transfer properties. The recorded cyclic voltammograms (Fig. 7A) are plain GCE (a), graphene oxide (b), CSGO composite (c) and CSCFGO composite (d) at pH 7.0 at scan rate 50mVs^{-1} for 0.1mM of L-dopa. The cyclic voltammograms shows anodic peak corresponding to the transformation of L-dopa to Dopamine Quinone. A small oxidation and reduction peak was observed for L-dopa at plain GCE (curve a), medium current response at graphene oxide modified electrode (curve b), whereas (curve c) very good response current was noted but the potential was shifted to higher potential. So, we chose to entrapment process it shows a very good higher current response than the other modified electrode was observed (curve d). The L-dopa and the formed *o*-quinone on the surface of modified electrode undergo quasi-reversible two-electron process. This CV demonstrated that the CSCFGO enhanced the conductivity of the composite and led to a faster electron transfer. From the cyclic voltammetric study it is concluded that CSCFGO modified electrode has resulted in higher sensitive electrode for the determination of L-dopa.

To measure the L-dopa by using the CSCFGO electrode is based on that the generated by the oxidation of L-dopa it is directly proportional to the L-dopa concentration in the solution. Fig. 7B shows the DPV response current experiment with L-dopa concentration in pH 7.0 of the electrochemical sensor under control stirred condition has a much higher current sensitivity and the relationship is between response current and L-dopa concentration in buffer pH 7.0 in room temperature. Under this condition it is used to estimate the detection limit of L-dopa. Figure. 7C shows the response current gives the L-dopa concentration a linear range of 1×10^{-7} to $3 \times 10^{-5}\text{M}$ and the lower limit of detection and sensitivity are $0.5 \times 10^{-7}\text{M}$ and $7.34\mu\text{A}$, respectively. Inset of Fig. 7C, a plot of inverse of current and substrate concentration was calculated from Fig. 7C. The catalytic reaction is called first-order reaction, response current increases slowly the concentration increases and attains steady state and it becomes zero-order kinetics [22]. At the resultant experimental the results showed that the methods were simple and rapid with high accuracy. The prepared electrode was compared with already existing electrode (Table 1) [23-30]. CSCFGO electrode shows significant towards L-dopa.

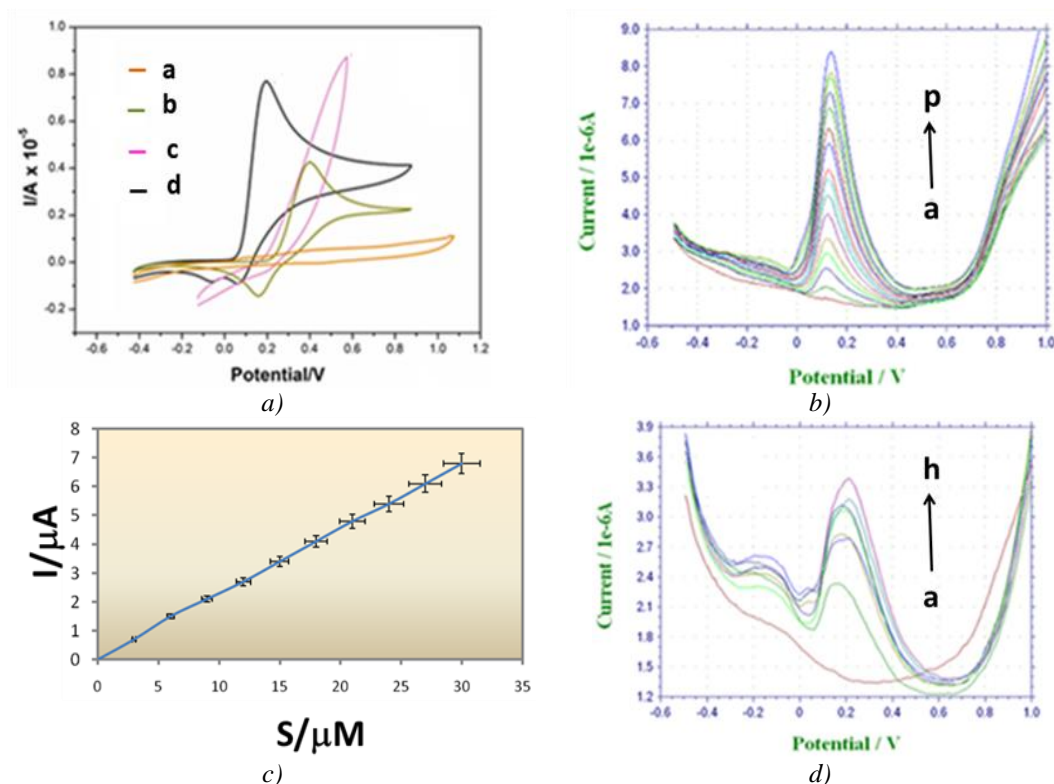


Fig.7. A Cyclic Voltammetry response of 0.1mM of L-dopa for GCE (a), Graphene oxide modified electrode (b), CSGO composite (c) CSCFGO composite (d). B) DPVs of CSCFGO composite electrode for L-dopa concentrations buffer, 2, 4, 6, 8, 10, 12, 14, 16,18, 20, 22, 24, 26, 28 and 30 μ M. C) Correlation between response current and L-dopa concentration at pH 7.0 and 25.0 $^{\circ}$ C Inset (Correlation between response current and L-dopa concentration at pH 7.0 and 25.0 $^{\circ}$ C. The plots of I/I against $1/[S]$ according to the data in the figure 7C). D) Effect of interference on the response of the L-dopa sensor buffer, 5 μ M, 10 μ M, 5 μ M Ascorbic acid, 15 μ M, 5 μ M D-glucose, 5 μ M L-glutamic acid.

Table 1. Comparison of this work previous reports of L-dopamine detection.

S.No	Electrode Materials	Linear Range	Lower limit of Detection	Ref
1.	CuHSA/GPE	1.0×10^{-4} to 8.0×10^{-4}	5.27×10^{-5}	23
2.	GRP-SIALNB-MB / GPE	5.0×10^{-6} to 5.0×10^{-4}	1.49×10^{-6}	24
3.	PbO ₂ immobilized in Polyester/GPE	2.6×10^{-4} to 1.2×10^{-3}	2.50×10^{-5}	25
4.	BDDE	2×10^{-6} to 10×10^{-5}	0.8×10^{-6}	26
5.	ppy/trion/MWCNT/GCE	1×10^{-6} to 10×10^{-5}	0.1×10^{-6}	27
6.	Co(DMG) ₂ CIPy/MWCNT/BPPG	3×10^{-6} to 10×10^{-5}	0.86×10^{-6}	28
7.	ERGO/Poly-Gly/GCE	1×10^{-6} to 5×10^{-5}	0.15×10^{-6}	29
8.	Cysteic acid/GCE	3.5×10^{-6} to 9.6×10^{-5}	0.36×10^{-6}	30
9.	chitin base Graphene oxide/Co-Fe ₂ O ₃	1×10^{-7} to 3×10^{-5}	0.5×10^{-7}	This Work

The DPV responses of L-dopa in presence of potential interferences such as ascorbic acid, D-glucose and L-glutamic acid phosphate buffer pH 7.0 are presented in Fig. 7D. The interfering substances were added sequentially in the same solution and the DPV measurements were carried out. Since there is no significant change in the current response, the selectivity of the sensor is good. The response current was measured for 2 μ M L-dopa by employing the fabricated electrode. The electrode was washed with deionized water and kept for one week at 4°C. The response current was measured again and only 3-4% change in the response current was observed.

4. Conclusion

In this work, chitosan@Co-Fe₂O₃- Graphene oxide/ hybrid nanocomposites are prepared by chitin deacetylation method. As-prepared materials functional groups identified by FTIR. FTIR spectra was confirmed the chitosan, Graphene oxide and Co-Fe₂O₃ composite. The peak at 1651 cm⁻¹ -NH stretching vibration and 1115 cm⁻¹CO stretching vibration and 447cm⁻¹ which is attributed to the Co-Fe₂O₃ stretching vibration. The peak at 1576 cm⁻¹ -NH stretching vibration and 1119 cm⁻¹CO stretching vibration. The crystallite size of chitin base Graphene oxide-Fe₂O₃ and Graphene oxide/Co-Fe₂O₃composites was observed the size in the range of 16.54 and 19 nm, respectively. The surface morphology and particle size in nano of chitin base Graphene oxide/Co-Fe₂O₃hybrid nanocomposites were characterized by scanning electron microscopy (SEM). The composite electrode exhibit very sensitivity and selectivity for L-dopa. It can be seen that the charge curves almost linear and symmetrical to their discharge counterparts, indicating good electrochemical performance of the chitin base Co doped Graphene oxide/Fe₂O₃hybrid composites.

References

- [1] V. Subramanian, H. Zhu, R. Vajtai, P. M. Ajayan, B. Wei, *J. Phys. Chem. B* **109**, 20207 (2005).
- [2] A. L. Mohana, R. F. Estaline, A. Imran, J. S. Ramaprabhu, *Nanoscale Res. Lett.* **3**, 145 (2008).
- [3] A. Karina, C.-G. Monica, L.-C. Nieves, C.-P. Pedro, *Adv. Funct. Mater.* **15**, 1125 (2005).
- [4] S.-J. Bao, C. M. Li, C.-X. Guo, Y. Qiao, *J. Power Sources*, **180**, 676 (2008).
- [5] R. Kotz, M. Carlen, *Electrochim. Acta*, **45**, 2483 (2000).
- [6] S. Niyogi, E. Bekyarova, M. E. Itkis, J. L. McWilliams, M. A. Hamon, R. C. Haddon, *J. Am. Chem. Soc.* **128**, 7720 (2006).
- [7] L. Tang, Y. Wang, Y. Li, H. Feng, J. Lu, J. Li, *Adv. Funct. Mater.* **19**, 2782 (2009).
- [8] A. K. Geim, K. S. Novoselov, *Nature* **6**, 183 (2007).
- [9] H. S. Shin, K. Kim, A. Benayad, S. Yoon, H. Park, I.-S. Jung, M. Jin, H.-K. Jeong, J. Kim, J.-Y. Choi, *Adv. Funct. Mater.* **19**, 1987 (2009).
- [10] H. He, J. Klinowski, M. Forster, A. Lerf, *Chem. Phys. Lett.* **287**, 53 (1998).
- [11] A. Lerf, H. He, M. Forster, J. Klinowski, *J. Phys. Chem. B*, **102**, 4477 (1998).
- [12] S. Stankovich, R. D. Piner, S. T. Nguyen, R. S. Ruoff, *Carbon*, **44**, 3342 (2006).
- [13] H. K. Jeong, Y. P. Lee, R. J. W. E. Lahaye, M. H. Park, K. H. An, I. J. Kim, C. W. Yang, C. Y. Park, R. S. Ruoff, *J. Am. Chem. Soc.* **130**, 1362 (2008).
- [14] C. Zhou, S. Kumar, C. D. Doyle, J. M. Tour, *Chem. Mater.* **17**, 1997 (2005).
- [15] J. Y. Lee, K. H. An, J. K. Heo, Y. H. Lee, *J. Phys. Chem. B*, **107**, 8812 (2003).
- [16] A. L. M. Reddy, S. Ramaprabhu, *J. Phys. Chem. C*, **111**, 7727 (2007).
- [17] M. Kaempgen, C. K. Chan, J. Ma, Y. Cui, G. Gruner, *Nano Lett.* **9**, 1872 (2009).
- [18] H. Wang, Q. Hao, X. Yang, L. Lu, X. Wang, *Electrochem. Commun.* **6**, 1158 (2009).

- [19] X. Zhou, X. Huang, X. Qi, S. Wu, C. Xue, F. Y. C. Boey, Q. Yan, P. Chen, H. Zhang, *J. Phys. Chem. C*, **113**, 10842 (2009).
- [20] M. D. Stoller, S. Park, Y. Zhu, J. An, R. S. Ruoff, *Nano Lett.*, **8**, 3498 (2008).
- [21] S. Anandhavelu, V. Dhanasekaran, V. Sethuraman, Hui Joon Park, *J. Nanosci. Nanotechnol.* **16**, 1321 (2016).
- [22] V. Sethuraman, P. Muthuraja, J. A. Raj, P. Manisankar, *Biosens. Bioelectron.*, **84**, 112 (2016).
- [23] D. R. Silvestrini, T. F. S. Da Silveira, U. O. Bicalho, D. R. Do Carmo, *Int. J. Electrochem. Sci.* **10**, 2839 (2015).
- [24] J. F. Giarola, K. B. Borges, C. R. T. Tarley, F. M. de Oliveira, E. S. Ribeiro, A. C. Pereira, *Arab. J. Chem.* **10**, 430 (2017).
- [25] H. C. De Melo, A. P. D. Selegim, W. L. Polito, O. Fatibello-Filho, I. C. Vieira, *J. Braz. Chem. Soc.* **18**, 797 (2007).
- [26] Dalibor M Stanković, Anchalee Samphao, Biljana Dojcinović, Kurt Kalcher, *Acta Chim Slov.* **63**, 220 (2016).
- [27] S. Shahrokhian, E. Asadian, *J. Electroanal. Chem.* **636**, 40 (2009).
- [28] F. R. F. Leite, C. M. Maroneze, A. B. de Oliveira, W. T. P. dos Santos, F. S. Damos, R. C. Silva Luz, *Bioelectrochemistry*, **86**, 22 (2012).
- [29] V. N. Palakollu, N. Thapliyal, T. E. Chiwunze, R. Karpoormath, S. Karunanidhi, S. Cherukupalli, *Mater Sci Eng C*. **77**, 394 (2017).
- [30] Zahra Hassanvand, Fahimeh Jalali, *Mater Sci Eng C*. **98**, 496 (2019).